

(25) (Fig. 4B). In wild-type MEFs, GFP-RelA was principally expressed in the nucleus (panel a), whereas the coexpression of HDAC3 induced a cytoplasmic pattern of GFP-RelA epifluorescence (panel b). However, a very different pattern was obtained in the  $\text{I}\kappa\text{B}\alpha^{-/-}$  MEFs. Whereas GFP-RelA also exhibited a nuclear pattern of epifluorescence, the coexpression of HDAC3 in these  $\text{I}\kappa\text{B}\alpha^{-/-}$  MEFs failed to induce a cytoplasmic redistribution of RelA (panel d). Reconstitution of these  $\text{I}\kappa\text{B}\alpha^{-/-}$  cells by transfection with small quantities of an  $\text{I}\kappa\text{B}\alpha$  expression vector restored HDAC3-induced cytoplasmic expression of the GFP-RelA protein (panel f). In the absence of HDAC3, GFP-RelA remained principally nuclear, indicating that the levels of  $\text{I}\kappa\text{B}\alpha$  expressed were not sufficient on their own to produce cytoplasmic sequestration of GFP-RelA in these  $\text{I}\kappa\text{B}\alpha^{-/-}$  MEFs (panel e). These results indicate that  $\text{I}\kappa\text{B}\alpha$  is required for the nuclear export of deacetylated forms of RelA, which display increased binding of  $\text{I}\kappa\text{B}\alpha$ .

These findings reveal a new mechanism through which nuclear NF- $\kappa\text{B}$  function is regulated (Fig. 4C). RelA is subject to stimulus-coupled acetylation likely mediated through the p300 and CBP coactivators. One biological consequence of this modification is that acetylated

RelA becomes a very poor substrate for binding by newly synthesized  $\text{I}\kappa\text{B}\alpha$ . Whether p50 or perhaps  $\text{I}\kappa\text{B}\alpha$  are similarly subject to biologically important acetylation/deacetylation reactions remains to be explored. Our studies identify acetylated RelA as a novel nonhistone substrate of HDAC3. As such, HDAC3-mediated deacetylation functions as an intranuclear molecular switch that when activated initiates a series of events culminating in the termination of the NF- $\kappa\text{B}$  transcriptional response. The  $\text{I}\kappa\text{B}\alpha$ -dependent nuclear export of the HDAC3-deacetylated RelA-containing complexes also serves to replenish the depleted cytoplasmic pool of latent NF- $\kappa\text{B}$ - $\text{I}\kappa\text{B}\alpha$  complexes needed for the next inductive NF- $\kappa\text{B}$  response in these cells.

References and Notes

1. A. S. Baldwin Jr., *Annu. Rev. Immunol.* **14**, 649 (1996).
2. S. Ghosh, M. J. May, E. B. Kopp, *Annu. Rev. Immunol.* **16**, 225 (1998).
3. M. Karin, *Oncogene* **18**, 6867 (1999).
4. N. D. Perkins et al., *Science* **275**, 523 (1997).
5. M. O. Hottiger, L. K. Felzien, G. J. Nabel, *EMBO J.* **17**, 3124 (1998).
6. K. A. Sheppard et al., *Mol. Cell. Biol.* **19**, 6367 (1999).
7. H. Zhong, R. E. Voll, S. Ghosh, *Mol. Cell* **1**, 661 (1998).
8. A. Imhof, A. P. Wolffe, *Curr. Biol.* **8**, 422 (1998).
9. D. E. Sterner, S. L. Berger, *Microbiol. Mol. Biol. Rev.* **64**, 435 (2000).
10. M. T. Kouzarides, *EMBO J.* **19**, 1176 (2000).
11. H. Kuo, C. D. Allis, *Bioessays* **20**, 615 (1998).

12. W. D. Cress, E. Seto, *J. Cell Physiol.* **184**, 1 (2000).
13. H. H. Ng, A. Bird, *Trends Biochem. Sci.* **25**, 121 (2000).
14. S. C. Sun, P. A. Ganchi, D. W. Ballard, W. C. Greene, *Science* **259**, 1912 (1993).
15. K. Brown, S. Park, T. Kanno, G. Franzoso, U. Siebenlist, *Proc. Natl. Acad. Sci. U.S.A.* **90**, 2532 (1993).
16. A. A. Beg, T. S. Finco, P. V. Nantermet, A. S. Baldwin Jr., *Mol. Cell. Biol.* **13**, 3301 (1993).
17. F. Arenzana-Seisdedos et al., *Mol. Cell. Biol.* **15**, 2689 (1995).
18. F. Arenzana-Seisdedos et al., *J. Cell Sci.* **110**, 369 (1997).
19. Supplementary figures and information on experimental protocols are available on Science Online at [www.sciencemag.org/cgi/content/full/293/5535/1653/DC1](http://www.sciencemag.org/cgi/content/full/293/5535/1653/DC1).
20. H. Bogerd, W. C. Greene, *J. Virol.* **67**, 2496 (1993).
21. E. Soutoglou, N. Katrakili, I. Talianidis, *Mol. Cell* **5**, 745 (2000).
22. C. Spilianakis, J. Papamatheakis, A. Kretsovali, *Mol. Cell. Biol.* **20**, 8489 (2000).
23. M. Yoshida, S. Horinouchi, *Ann. N. Y. Acad. Sci.* **886**, 23 (1999).
24. L.-F. Chen, W. C. Greene, unpublished data.
25. J. F. Klement et al., *Mol. Cell. Biol.* **16**, 2341 (1996).
26. We thank R. Goodman (Vollum Institute) and Y. Nakatani (NIH) for reagents; J. F. Klement (Jefferson Medical College) for providing the  $\text{I}\kappa\text{B}\alpha^{-/-}$  MEF cells; and A. O'Mahony for helping establish cultures of these cells. We also thank J. Carroll for assistance in the preparation of the figures and R. Givens for assistance in the preparation of the manuscript. Supported in part by funds provided by the J. David Gladstone Institutes, Pfizer, and the University of California, San Francisco-Gladstone Institute of Virology and Immunology Center for AIDS Research (P30MH59037).

8 May 2001; accepted 3 July 2001

## Allosteric Activation of a Spring-Loaded Natriuretic Peptide Receptor Dimer by Hormone

Xiao-lin He, Dar-chone Chow, Monika M. Martick, K. Christopher Garcia\*

Natriuretic peptides (NPs) are vasoactive cyclic-peptide hormones important in blood pressure regulation through interaction with natriuretic cell-surface receptors. We report the hormone-binding thermodynamics and crystal structures at 2.9 and 2.0 angstroms, respectively, of the extracellular domain of the unliganded human NP receptor (NPR-C) and its complex with CNP, a 22-amino acid NP. A single CNP molecule is bound in the interface of an NPR-C dimer, resulting in asymmetric interactions between the hormone and the symmetrically related receptors. Hormone binding induces a 20 angstrom closure between the membrane-proximal domains of the dimer. In each monomer, the opening of an interdomain cleft, which is tethered together by a linker peptide acting as a molecular spring, is likely a conserved allosteric trigger for intracellular signaling by the natriuretic receptor family.

The natriuretic peptides (NPs) are three homologous peptide hormones that play important roles in the maintenance of cardiovascular homeostasis, blood pressure, and body fluid regulation (i.e., natriuresis) (1). Collectively, these hormones function as an endogenous counterbalance to the renin-angioten-

sin/aldosterone system, as well as the hypothalamic/pituitary/adrenal axis. The three members of this family are atrial (ANP) and brain (BNP) natriuretic peptides, which are produced by the heart; and CNP, which is expressed in endothelial cells (1). ANP and BNP are thought to be the primary regulators

of peripheral natriuretic activity; CNP is present mainly in the brain. ANP, BNP, and CNP are highly homologous (~70% identical) and share as a common motif a 17-amino acid loop formed by a disulfide bond (Fig. 1). The lack of defined structure(s) in solution and the questionable relevance of "lowest energy" solution conformations to the receptor-bound conformation of peptide hormones mean that assessing the bioactive conformations of these peptides remains a general problem (2).

The actions of the NPs are mediated by three homologous single-transmembrane, glycosylated cell-surface receptors (NPR-A, -B, and -C) (3-5). These receptors possess about 30% homologous extracellular ligand-binding domains (ECDs) (~450 amino acids) with conserved topologies but possess different downstream activation mechanisms. NPR-C is the most promiscuous of the receptors, binding to all NPs with high affinity, whereas NPR-A and NPR-B are more specific for ANP and CNP, respectively (6). In the cases of NPR-A and NPR-B, hormone binding to the ECDs results in the production of intracellular cyclic guanosine 3',5'-monophosphate by a guanylyl-cyclase activity that resides in the intracellular domains (5, 7). For NPR-C, which represents over 95% of NPR in vivo, ligand binding results in both internalization and degradation (i.e., clearance), as well as signaling by heterotrimeric GTP-

## REPORTS

binding protein-mediated phosphoinositide hydrolysis and inhibition of adenylyl cyclase (8, 9). The clearance function serves to buffer NP-mediated changes in blood pressure, and the signaling function can suppress catecholamine release (10–12). The NPR-C cytoplasmic tail is phosphorylated upon hormone engagement of the ECD, activating  $G_i$ -like proteins in a fashion similar to the insulin-like growth factor-II receptor (13).

Despite their different downstream activation cascades, the molecular mechanisms of hormone recognition and receptor activation are likely to be conserved throughout this family because of the high degree of similarity found among the receptors and ligands (8, 14). A number of key issues, such as the ligand:receptor stoichiometry, the roles of oligomerization and conformational change, and the importance of glycosylation remain controversial (1, 4, 5, 15–19). It is clear that a simple ligand-induced oligomerization is not sufficient for activation. The signaling of the NPR appears highly sensitive to mutations of the membrane-proximal portion of the ECD; it is generally assumed that hormone binding induces conformational changes in this region as a means of activation (3, 20–22). Another unique feature of this receptor family is that glycosylation appears to be

important for modulating the binding activity of the extracellular domains (23–26).

We have attempted to resolve some of these structural issues by carrying out biophysical studies of a soluble form of the NPR-C ectodomain that recapitulates the ligand pharmacology of the receptor on the cell surface. ANP, BNP, and CNP bind to NPR-C with a 1:2 hormone:receptor stoichiometry and enthalpy-driven energetics. We have also determined the crystal structures of both the unliganded and CNP-complexed forms of the receptor ECD, which reveal a large-scale conformational change that is likely a conserved extracellular activation trigger for members of the NPR family.

We expressed the extracellular domains of both human NPR-A and NPR-C receptors in *Drosophila melanogaster* cells so that glycosylated receptors were used for biochemical and crystallographic studies (27, 28). Both soluble receptor ECDs eluted as dimers on gel filtration, and both exhibited quantitative band-shifting by substoichiometric (~1:2) amounts of NP hormones in a nondenaturing native gel experiment. We measured the ligand:receptor stoichiometry and binding thermodynamics (enthalpy  $\Delta H$ , entropy  $\Delta S$ , and free energy  $\Delta G$ ) for the interaction of NPR-C with ANP, BNP, and CNP using isothermal titration calorimetry (ITC) (Fig. 1) (29). NPR-C binds to all NPs with a clear 2:1 stoichiometry, and all the hormones bind with strongly enthalpy-driven thermodynamics and unfavorable entropy (Fig. 1) (30). The affinities are  $K_d \leq 1$  nM for CNP and ANP ( $K_d$ , dissociation constant), and the rank order

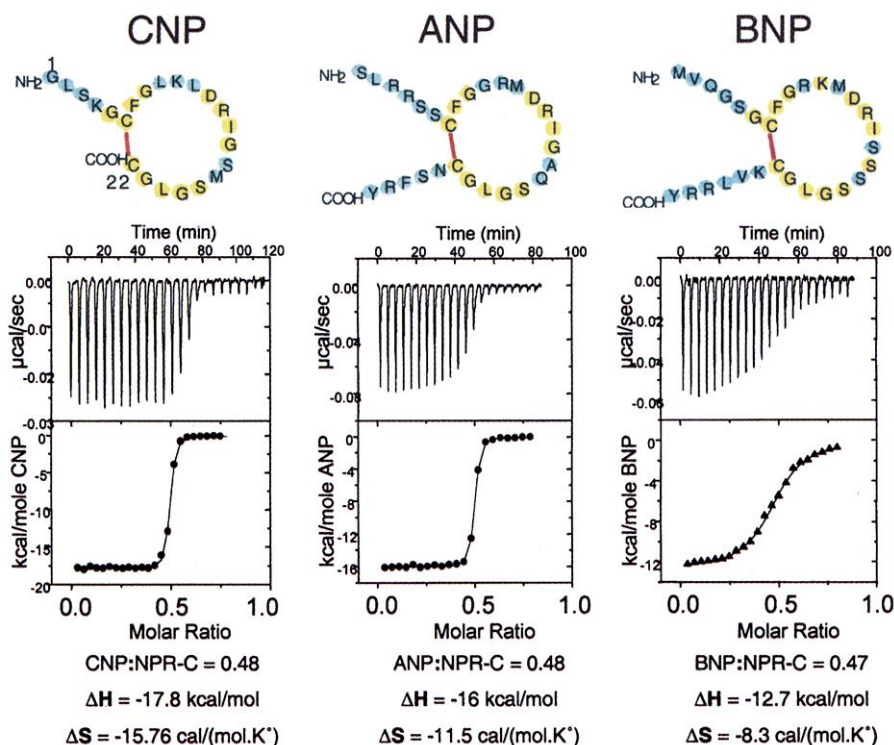
of affinities is  $CNP \approx ANP \gg BNP$  (Fig. 1), which mimics the pharmacology of the naturally occurring receptor (6). The strong enthalpy-driven binding ( $-10$  to  $-18$  kcal/mol) implies the formation of high-energy polar contacts between hormone and NPR-C, and the unfavorable (negative) entropic energy barrier is likely due to the substantial conformational chain entropy of the flexible peptide in solution (31).

We crystallized NPR-C both unliganded and bound to CNP (Table 1). The unliganded structure was determined to 2.9 Å with one receptor ECD, or a half-dimer in the asymmetric unit, with the second half of the dimer related by a crystallographic twofold axis (Fig. 2A). The structure was determined by molecular replacement with a truncated model derived from a monomer of the unliganded rat NPR-A structure (22). Each monomer is dumbbell-shaped, with each domain adopting an  $\alpha\beta$  fold consisting of a central  $\beta$  sheet surrounded by  $\alpha$  helices (Fig. 2, A and B). This fold is similar to that found in bacterial periplasmic-binding proteins (bPBPs) (e.g., the leucine-isoleucine-valine binding protein LIVBP), and to the unliganded rat NPR-A structure (22, 32). The membrane-distal and membrane-proximal ( $NH_2$  and  $COOH$ ) domains are connected by three short connecting peptides, which form a hinge with an “elbow angle” ( $\sim 120^\circ$ ) analogous to that seen in type I bPBPs. The hinge forms a cleft between the two domains (Fig. 2A), which is the ligand binding site for bPBPs (32). In the NPR-C structure, we see ordered, high-mannose carbohydrate chains emanating from

Departments of Microbiology and Immunology and Structural Biology, Stanford University School of Medicine, Fairchild D319, 299 Campus Drive, Stanford, CA 93405-5124, USA.

\*To whom correspondence should be addressed. E-mail: kcgarcia@stanford.edu

**Fig. 1.** Thermodynamics and 1:2 stoichiometry of NP interactions with human NPR-C. The ITC of interactions of NPR-C with CNP, ANP, and BNP is shown from left to right. The sequences of CNP, ANP, and BNP are portrayed in schematic form showing the cyclic peptides with the invariant residues colored yellow and the different residues colored blue. The measured thermodynamic ( $\Delta H$  and  $\Delta S$ ) and stoichiometric ( $N$ ) values are indicated below. The top panel is the raw data and the bottom panel is the plot of heat changes against the ratio of peptide hormone to receptor for each injection. The solid curve is the best-fit curve with nonlinear least-squares fitting. The negative  $\Delta H$  and  $\Delta S$  ( $T$ , temperature) show that the interactions are strongly enthalpy-driven and entropically unfavorable. The  $N$  of 0.5 is evidence of that one peptide hormone binds to two receptor monomers. The overall  $K_d$  (and  $\Delta G$ ) is too low (i.e., high affinity) for precise quantitation by ITC; however, approximate values calculated from these data are CNP,  $K_d \sim 0.45$  nM; ANP,  $K_d \sim 0.95$  nM; and BNP,  $K_d \sim 47.5$  nM (actual  $K_d$  values would be lower). This rank order of affinities matches the order of affinities measured on cells bearing NPR-C. Further details of the ITC are given in (30).



two out of the four possible N-linked glycosylation sites (Asn<sup>248</sup> and Asn<sup>349</sup>) (Figs. 2 and 3) [Web fig. 1 (33)].

The uncomplexed NPR-C dimer orientation (Fig. 2A) is different from a tail-to-tail dimer that was observed in the uncomplexed rat NPR-A crystal structure and was proposed to be physiologically relevant (22) [(Web fig. 2 (33))]. The NPR-C dimer is mediated through the NH<sub>2</sub>-terminal domains, which form a

complementary four-helix bundle hydrophobic dimer interface (1378 Å<sup>2</sup> of the buried surface area), with the dimer twofold running through the center of the four helices (Fig. 2) [Web figs. 1 and 2 (33)]. The dimeric interface has a large, continuous hydrophobic core, including the residues Phe<sup>69</sup>, Leu<sup>68</sup>, Leu<sup>101</sup>, Trp<sup>105</sup>, Val<sup>72</sup>, Ala<sup>76</sup>, and Val<sup>75</sup>; and the aliphatic atoms of His<sup>105</sup>, Asn<sup>65</sup>, and Arg<sup>100</sup> from each mono-

mer [Fig. 2, Web fig. 1 (33)]. The helical bundle is flanked by six symmetric hydrogen bonds (three H bonds from each side), consisting of Asp<sup>73</sup>Oδ2-Trp<sup>104</sup>Ne1, Asp<sup>73</sup>Oδ1-His<sup>105</sup>Nδ2, and Asn<sup>65</sup>Nδ2-Glu<sup>125</sup>Oε2. The H-bonding residues Asp<sup>73</sup>, Trp<sup>104</sup>, and His<sup>105</sup> are completely conserved across the NPR family, and the hydrophobic core residues in the dimer interface are also either conserved or have conservative substitutions. This dimer places the ligand-binding sites within the interdimer interface, consistent with the measured stoichiometry. The NPR-A tail-to-tail dimer is mediated through an interface between the COOH-terminal domains, which results in the proposed ligand-binding regions facing opposite directions and thus accommodating a proposed 2:2 stoichiometry (22). Because the stoichiometry of the NPR appears to be 1:2, the NPR-A tail-to-tail dimer is probably not physiologically relevant [Web fig. 2 (33)].

We crystallized the complex of NPR-C with CNP and determined the structure to 2.0 Å resolution (Table 1). The conformation of the NH<sub>2</sub>-terminal domain dimeric interface is unchanged (Figs. 2B and 3). A single CNP molecule is bound in the center of the twofold symmetric dimeric receptors (Figs. 2B and 4), confirming the ITC determination of the 1:2 stoichiometry (Fig. 1). Because the hormone is bound exactly along the center of the receptor dimeric twofold axis, the electron density shows the average of two equally occupied, twofold symmetric orientations of this conformation imposed by the dimeric receptor (Table 1) [Web fig. 1 (33)].

The peptide adopts a disk-like conformation, in which the narrowest dimension intercalates between the two halves of the dimer. The gap between the two COOH-terminal domains closes by 20 Å, so that the two monomers make intimate contact with opposing faces of the peptide (Figs. 2 and 3). The closure of the membrane proximal domains onto the peptide causes the elbow angle between the NH<sub>2</sub>-terminal and COOH-terminal domains of each monomer to open by ~13.5° (Fig. 3). Thus, the receptor appears to have "open" and "closed" states, which are regulated by hormone binding. This is analogous to, but the converse of, the soluble bPBPs' hinge-movement transition to a closed state upon ligand binding within the cleft (34). Here, CNP does not bind within the cleft between the domains to close the structure but rather opens the interdimer cleft by binding to the opposite side of the monomer (Fig. 3). Hence, it appears that the malleable architecture of the bPBPs has been used by the NPR family to transduce a ligand-induced allostery in a cell-surface receptor, but with a different switching mechanism. Mutants of NPR-A that are disulfide-bridged into

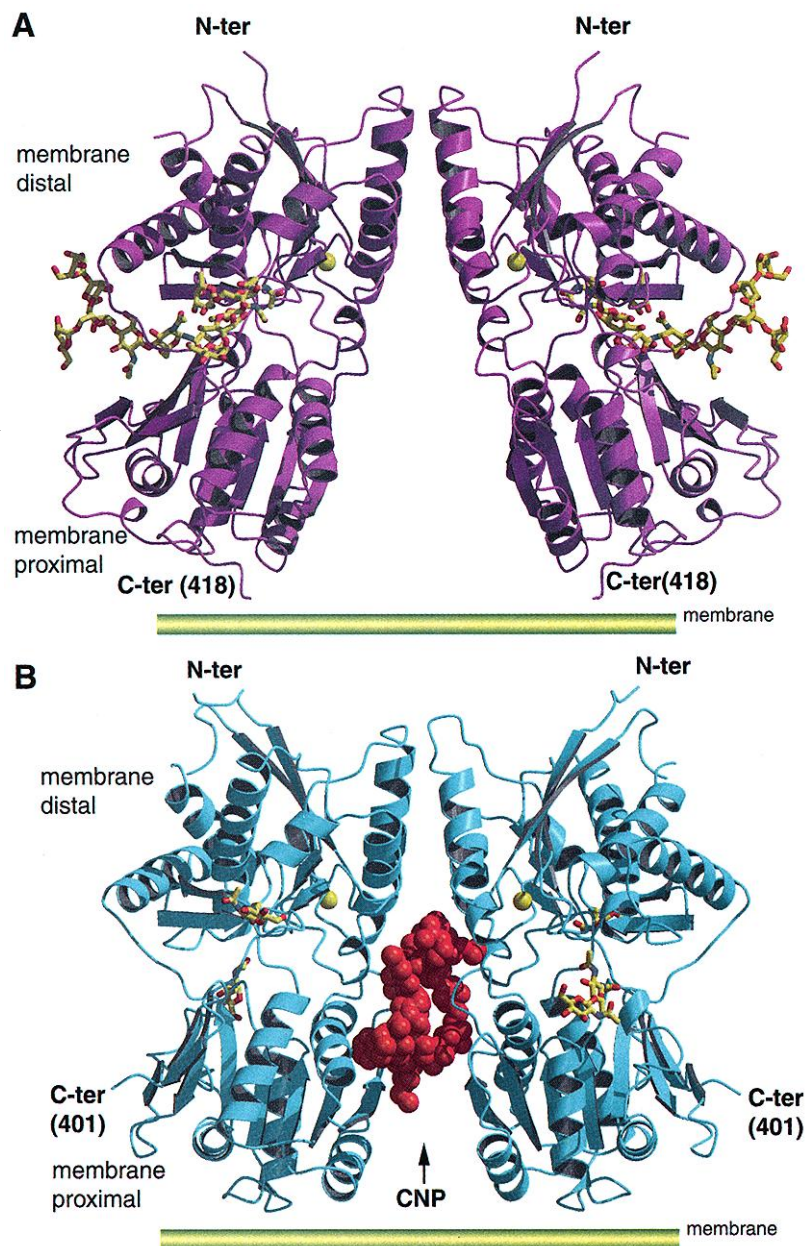


**Fig. 2.** Three-dimensional structures of human NPR-C and the NPR-C/CNP complex. Shown are ribbon diagrams of (A) the unliganded NPR-C dimer (top, in magenta) and of (B) NPR-C bound to human CNP (bottom, in cyan with orange CNP hormone in space-filling view). The cell surface is shown in schematic at the base of the COOH-termini of both receptors (on the cell surface, the receptor ECD would enter the membrane bilayer at about residue 430). The twofold axis relating each monomer in both the free and liganded complex runs directly through the center of the dimer, parallel to the page. The carbohydrates are drawn as yellow sticks. The large Asn<sup>248</sup>-linked glycan (six moieties) is especially clear in the unliganded structure between the membrane-proximal (NH<sub>2</sub>-terminal, N-ter) and membrane-distal (COOH-terminal, C-ter) domains of the dumbbell-shaped monomers. The figure was drawn with BOBSCRIPT and rendered with RASTER3D (41).

REPORTS

**Fig. 3.** Conformational changes in the NPR-C complex and the molecular spring. **(A)** Backbone representations of bound (cyan) versus unliganded (purple) NPR-C (the peptide in the middle is shown in red). At the base of the structures, the width of the gap separating the COOH-terminal domains of the dimer in bound versus free form is indicated. The identical amino acid closest to the COOH-terminal at the base of the gap (Ala<sup>208</sup>) was used in both structures as the point from which to measure the gap to the dimeric-related residue (Ala<sup>208\*</sup>). For the elbow angle of the structures, identical reference points (a vector defining an  $\alpha$  helix in the membrane-distal and -proximal domains) were chosen in bound versus free structures from which to measure an interdomain angle. **(B)** The spring tethering the membrane-distal and -proximal domains in each monomer is stretched and lengthened by 2.5 Å in the bound structure (40). A ribbon representation is shown of the linker peptide, along with the secondary structure elements leading up to and away from the peptide. The loose structure of the unbound peptide is obvious as compared with the straightened peptide in the complex. **(C)** The N-linked glycan at Asp<sup>248</sup> forms extensive interactions with the linker peptide, which are broken upon hormone binding and conformational change (40). A stick representation of the peptide, the N-linked glycan, and the surrounding amino acids is shown. We have superimposed the Fo-Fc SIGMAA-weighted omit maps, at 2.9 Å (left) and 2.0 Å (right) of the NH<sub>2</sub>-linked glycan, to demonstrate the clarity of the carbohydrate conformational change.

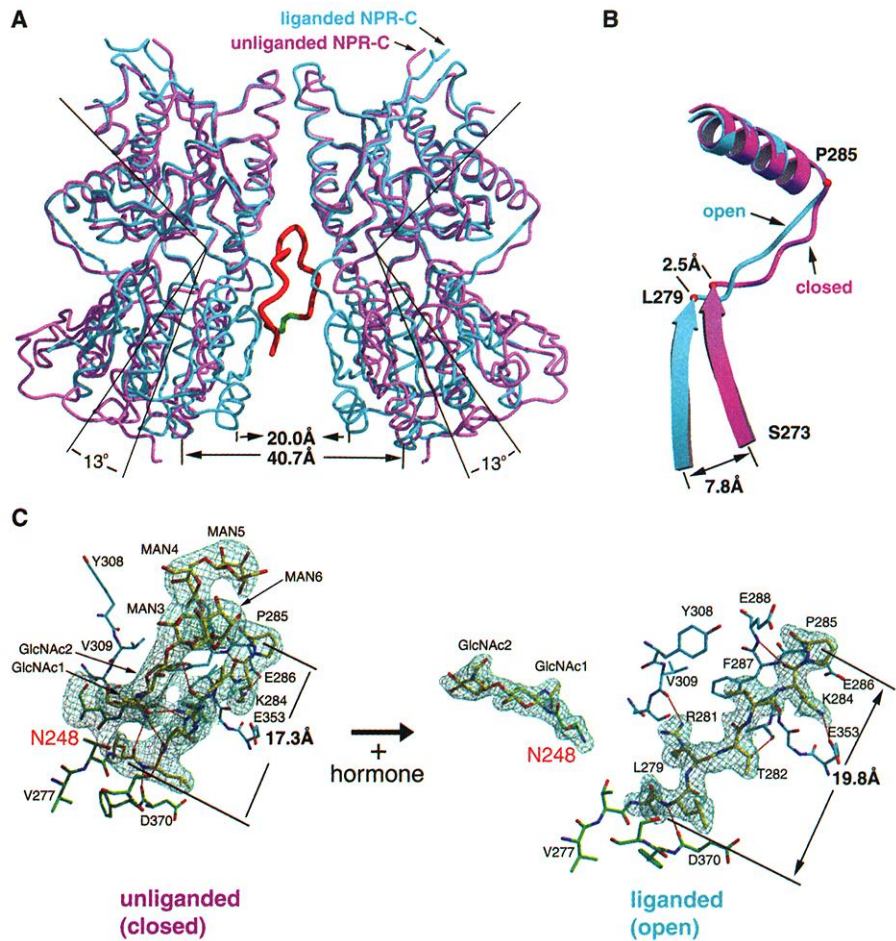
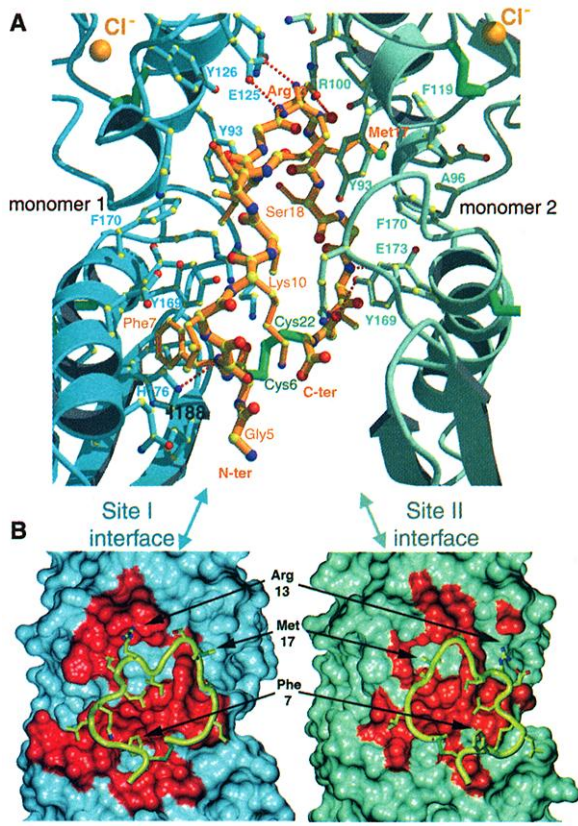


**Fig. 4.** Asymmetry of the hormone/receptor interfaces and the conformation of CNP. **(A)** Stick representation of the bound CNP peptide (orange) and the interacting amino acids from each NPR-C monomer (cyan and green) (40). The yellow spheres represent the bound chloride ions in each monomer. Ile<sup>188</sup>, which has been shown to modulate the ligand pharmacology of NPR-C (37), is next to the CNP residue Phe<sup>7</sup>, and is labeled in black. **(B)** This interface is then shown in an "open-book" view of the molecular surface of each receptor monomer. The CNP peptide is shown as a yellow backbone-and-stick model projected onto the respective buried surfaces (red patches) of each NPR-C monomer. The figures were drawn with BOBSCRIPT, RASTER3D, and VMD (47).



homodimers through the juxtamembrane stalk are constitutively active, suggesting that the closure of the interdimer gap is associated with activation (21). Numerous other functional studies have also implicated the COOH-terminal region of the ECD as being critical for ligand-induced signaling in this family (15, 21, 35, 36).

In the unliganded structure, the linker peptide between the NH<sub>2</sub>- and COOH-terminal domains is stabilized by nine H bonds [five with the Asn<sup>248</sup>-linked carbohydrate moieties and four with the surrounding protein structure (Lys<sup>284</sup>O-Glu<sup>287</sup>N; Lys<sup>284</sup>NZ-Glu<sup>286</sup>Oe2; Asn<sup>281</sup>N-<sup>372</sup>Oγ; Asp<sup>370</sup>O-Leu<sup>280</sup>N)] (Figs. 2 and 3).

In the complex, the opening of the interdomain elbow angle results in a lengthening of this six-residue peptide by ~2.5 Å, which substantially straightens its structure (Fig. 3B). Moreover, all but one of the H-bonding contacts stabilizing this peptide in the unliganded structure are broken, and four new H bonds form to give the set of H bonds Lys<sup>284</sup>O-Glu<sup>353</sup>N, Thr<sup>282</sup>Oγ1-Ala<sup>356</sup>O, Arg<sup>281</sup>Nη2-Val<sup>309</sup>O, Asp<sup>370</sup>O-Leu<sup>280</sup>N, and Lys<sup>284</sup>N-Glu<sup>288</sup>N (Fig. 3C). The four H-bonding contacts with the Asn<sup>248</sup>-linked glycan are broken and the sugar becomes largely disordered (Fig. 3C). Thus, the linker peptide appears to act as a

REPORTS

**Table 1.** Crystallographic statistics for unliganded NPR-C and the NPR-C/CNP complex. The human NPR-C receptor extracellular domain (430 amino acids) was secreted from *D. melanogaster* cells, and the COOH-terminal hexa-histidine tag was removed with carboxypeptidase-A (40). Crystals of unliganded NPR-C were grown from 1.5 M sodium/potassium phosphate or 1.5 M potassium phosphate (pH 7.5) and cryo-cooled in the presence of 20% ethylene glycol. For the complex, NPR-C was incubated with an excess of human CNP and then purified by gel filtration chromatography. Crystals of the complex were grown from 0.8 M sodium citrate (pH 7.5) and were cryo-cooled in 20% glycerol. Data from a single crystal for both unliganded and complex were collected at SSRL BL9-2 and 9-1, respectively, and processed with MOSFLM and SCALA (47). The higher resolution NPR-C/CNP complex was solved first by molecular replacement (MR) with the coordinates of the unliganded ECD of rat NPR-A (Protein Data Bank accession code, 1DP4) (22). Only MOLREP (47) identified correct solutions with a polyalanine model. The two receptor monomers were refined in the early stages with NCS restraints, which were then released to allow for differences on surface loops. The hormone CNP was traced in a single unique conformation in two equally occupied twofold symmetric orientations, reflecting its location along the receptor dimer twofold. The peptide was refined in two orientations with equal occupancy (0.5) to satisfactory stereochemical criteria, with all but one (Met<sup>17</sup>) residue falling within favored or allowed regions of the Ramachandran plot as determined by PROCHECK (47). The unliganded NPR-C structure was solved by MR with the separate NH<sub>2</sub>- and COOH-terminal domains of the refined NPR-C complex. Both liganded and unliganded structures were refined with a maximum-likelihood target function, rigid-body refinement, cycles of simulated annealing with torsion angle molecular dynamics, and iterations between positional and B-factor minimization. SIGMAA-weighted 2Fo-Fc and omit Fo-Fc maps (CNS) were manually rebuilt in the program O, and stereochemical analysis was performed with PROCHECK (47). All data were used without truncation, except for 5% data randomly selected for cross validation. In the unliganded structure, two asparagine-linked glycosylation sites contained electron density for a total of 11 glycan residues (6 for Asn<sup>248</sup>, 5 for Asn<sup>349</sup>). In the NPR-C/CNP complex, we modeled a total of five N-linked glycan moieties on two N-linked sites in each monomer (Asn<sup>248</sup> and Asn<sup>349</sup>). In both structures, one chloride ion was clearly defined in each monomer.

	Unliganded NPR-C	NPR-C/CNP complex
<i>Data</i>		
Space group	P6 <sub>1</sub> 22	P2 <sub>1</sub> 2 <sub>1</sub> 2 <sub>1</sub>
Unit cell (Å) (a, b, c)	217.19, 217.19, 130.98	56.80, 136.46, 137.59
Matthews coefficient (Å <sup>3</sup> /dalton)	7.4	2.2
Source	SSRL, BL9-2	SSRL, BL9-1
Resolution (Å) (highest resolution shell)	50.0–2.9 (3.0–2.9)	50.0–2.0 (2.07–2.0)
Measured reflections	217,841	225,890
Unique reflections	43,722	70,832
Completeness (%)	98.1 (98.4)	97.7 (96.6)
I/σ(I)	7.4 (2.0)	6.7 (1.6)
R <sub>merge</sub> * (%)	8.1 (43.5)	7.4 (44.8)
<i>Refinement statistics</i>		
Resolution range (Å)	50.0–2.9 (3.0–2.9)	50.0–2.0 (2.07–2.0)
R <sub>cryst</sub> †	0.243 (0.367)	0.227 (0.330)
R <sub>free</sub> ‡	0.256 (0.389)	0.248 (0.343)
Average B factors (Å <sup>2</sup> )		
NPR-C	66.7	42.4
CNP	–	72.9
Oligosaccharides	82.5	82.7
Waters	–	46.0
Chlorides	34.9	30.6
Root mean square deviation from ideality		
Bond lengths (Å)	0.009	0.009
Bond angles (°)	1.4	1.5
Bonded B factors (Å <sup>2</sup> ) (main chain, side chain)	2.2, 3.2	1.9, 2.5
Ramachandran plot (%)		
(Favored, allowed, generous, disallowed)	85.9, 13.3, 0.8, 0	88.3, 11.2, 0.5, 0

\*R<sub>merge</sub> = Σ<sub>hkl</sub> |I - ⟨I⟩| / Σ<sub>hkl</sub>I, where I is the intensity of unique reflection hkl, and ⟨I⟩ is the average over symmetry-related observation of unique reflection hkl. †R<sub>cryst</sub> = Σ|F<sub>obs</sub> - F<sub>calc</sub>| / ΣF<sub>obs</sub>, where F<sub>obs</sub> and F<sub>calc</sub> are the observed and the calculated structure factors, respectively. ‡R<sub>free</sub> is R with 5% of reflections sequestered before refinement.

“molecular spring.” In concert with the N-linked glycan, it may help constrain the receptor in the closed conformation in the absence of ligand. The strong enthalpy of the hormone interaction (–19.8 kcal/mol) may be required to provide sufficient binding energy to destabilize the spring from its basal closed state.

The CNP conformation is nearly a circle in the bound state, with 18 of 22 hormone residues clearly visible (Figs. 2 and 4). The CNP NH<sub>2</sub>-terminal amino acids are largely disordered, suggesting a tenuous interaction of the CNP NH<sub>2</sub>-terminus with NPR-C. The peptide chain is fairly extended, with no in-

trapeptide H bonds formed, suggesting it will not be an energetically stable solution conformation in the unbound state. The conformation of the bound CNP does not resemble a solution structure of a conformationally constrained variant of ANP determined by nuclear magnetic resonance (2). In the bound state, the invariant bulky side chains of Phe<sup>7</sup>, Met<sup>17</sup>, and Arg<sup>13</sup> fix the interactions with NPR-C. The peptide is oriented with the disulfide bond and with NH<sub>2</sub>- and COOH-termini pointing downward (Fig. 4) toward the receptor COOH-terminal region, leaving ample space to accommodate the side chains of additional COOH-terminal ANP and BNP residues that occur in these hormones and that contribute to their receptor specificity (35).

There are numerous polar and hydrophobic interactions between CNP and each of the two NPR-C monomers (Fig. 4) (Web table 1) (hereafter designated site I and site II for receptor monomers 1 and 2, respectively). Although the dimeric receptor has twofold symmetry, the site I and site II hormone contacts are entirely different on both receptor and peptide, reflecting the asymmetry of the hormone sequence and structure (Fig. 4). The site I interface is more extensive than site II, but both sites are primarily composed of the COOH-terminal domains (Figs. 2 and 4), consistent with the allosteric activation mechanism transduced through movement of the juxtamembrane domains. The CNP Phe<sup>7</sup> side chain is in a large hydrophobic cavity bordered by NPR-C Ile<sup>188</sup>, which has been mapped in functional studies to determine the hormone pharmacology of NPR-C (8, 37). The key site I contact residues, CNP Phe<sup>7</sup>, Gly<sup>8</sup>, and Arg<sup>13</sup>, are conserved across all NP hormones (Fig. 1) and so likely represent common contacts. Site I and site II NPR-C residues contact CNP through numerous conserved residues shared between NPR-A, NPR-B, and NPR-C (Fig. 4) [Web table 2 (33)]. Collectively, the subset of hormone-contacting residues in NPR-C has a higher homology than the overall sequence homologies between the entire NPR receptor ECDs, indicating common ligand interaction modes [Web table 2 (33)].

NPR-C binds to all NPs, whereas NPR-A and NPR-B are more specific for ANP and CNP, respectively. The invariant receptor-contacting side chains of the three NP hormones would fix the basic binding geometry to the receptors, whereas the residues that differ between ANP, BNP, and CNP (mostly polar side chains with H-bonding potential) (Fig. 1) will likely form receptor subtype-specific contacts. The peptide interactions of the NPR appear similar in character to those between major

histocompatibility complex (MHC) antigens and antigenic peptides, which bind to a single MHC though a small subset of invariant "anchor" residues, whereas the nonanchor residues vary and dictate the T cell receptor specificity (38).

Two important issues that the NPR-C structures illuminate are (i) the role of glycosylation and (ii) the role of chloride ions. It has been demonstrated that glycosylation is necessary for full binding activity of NPR, although this fact remains controversial (23–26, 28). None of the N-linked glycans seen in the structure make direct contact with the ligand. It is most probable that the N-linked glycans serve an overall role in structural stabilization, and the effect on binding activity is indirect. Chloride has also been suggested to be required for receptor activity (39). We see a deeply bound chloride ion in each monomer in both the unliganded and complexed structures. This does not interact with the ligand and exhibits no surrounding conformational changes upon hormone binding, so this chloride is likely integral to the structural stability of the protein.

The NPR family has used an ancient protein fold, structurally predisposed to conformational flexibility, as a cell-surface signal transduction module. However, the mode of hormone interaction and allostery is without precedent. The presence of two nonidentical hormone interaction sites on the receptors substantially expands the scope of chemistries possible for the development of NPR-C antagonists for the treatment of cardiovascular diseases.

References and Notes

1. J. G. Drewett, D. L. Garbers, *Endocr. Rev.* **15**, 135 (1994).
2. W. J. Fairbrother, R. S. McDowell, B. C. Cunningham, *Biochemistry* **33**, 8897 (1994).
3. D. G. Lowe et al., *EMBO J.* **8**, 1377 (1989).
4. L. R. Potter, T. Hunter, *J. Biol. Chem.* **276**, 6057 (2001).
5. K. A. Lucaset al., *Pharmacol. Rev.* **52**, 375 (2000).
6. B. D. Bennett et al., *J. Biol. Chem.* **266**, 23060 (1991).
7. D. L. Garbers, D. G. Lowe, *J. Biol. Chem.* **269**, 30741 (1994).
8. A. M. Engel, D. G. Lowe, *FEBS Lett.* **360**, 169 (1995).
9. G. J. Trachte, S. Kanwal, B. J. Elmquist, R. J. Ziegler, *Am. J. Physiol.* **268**, C978 (1995).
10. M. B. Anand-Srivastava, *Biochemistry* **39**, 6503 (2000).
11. G. J. Trachte, *J. Pharmacol. Exp. Ther.* **294**, 210 (2000).
12. S. Takida, B. J. Elmquist, G. J. Trachte, *Hypertension* **33**, 124 (1999).
13. L. Pedro, R. Fenrick, M. Marquis, N. McNicoll, A. De Lean, *Mol. Cell. Biochem.* **178**, 95 (1998).
14. N. McNicoll, J. Gagnon, J. J. Rondeau, H. Ong, A. De Lean, *Biochemistry* **35**, 12950 (1996).
15. M. Itakura, H. Suzuki, S. Hirose, *Biochem. J.* **322**, 585 (1997).
16. K. S. Misono, N. Sivasubramanian, K. Berkner, X. Zhang, *Biochemistry* **38**, 516 (1999).
17. J. J. Rondeau et al., *Biochemistry* **34**, 2130 (1995).
18. D. G. Lowe, *Biochemistry* **31**, 10421 (1992).
19. J. T. Stults et al., *Biochemistry* **33**, 11372 (1994).
20. X. L. Rudner, K. K. Mandal, F. J. de Sauvage, L. A. Kindman, J. S. Almenoff *Proc. Natl. Acad. Sci. U.S.A.* **92**, 5169 (1995).
21. J. Labrecque, N. Mc Nicoll, M. Marquis, A. De Léan, *J. Biol. Chem.* **274**, 9752 (1999).
22. F. van den Akker et al., *Nature* **406**, 101 (2000).
23. D. G. Lowe, B. M. Fendly, *J. Biol. Chem.* **267**, 21691 (1992).
24. R. Fenrick, N. McNicoll, A. De Léan, *Mol. Cell. Biochem.* **165**, 103 (1996).
25. M. Hasegawa, Y. Hidaka, A. Wada, T. Hirayama, Y. Shimonishi, *Eur. J. Biochem.* **263**, 338 (1999).
26. M. Miyagi, X. Zhang, K. S. Misono, *Eur. J. Biochem.* **267**, 5758 (2000).
27. The coding sequences, including signal sequences (~40 amino acids), for the extracellular domains of human NPR-C (amino acids 1 through 475) and NPR-A (amino acids 1 through 472) were amplified by polymerase chain reaction to add COOH-terminal hexa-histidine tags and were subcloned into the pRMHa3 *D. melanogaster* expression vector. The cDNAs were individually cotransfected in S2 cells with a neomycin-resistance plasmid and selected for growth in G418-supplemented Schneider's expression media containing 10% fetal bovine serum. Stable transfectants were cloned by limiting dilution. For large-scale protein expression, the cell lines were expanded to 6 to 8 liters in spinner flasks at a density of 10<sup>7</sup> cells/ml in serum-free InsectXpress media (Biowhittaker, Gaithersburg, MD), at which point copper sulfate was added to a final concentration of 0.7 mM for 3 to 5 days. The supernatant was concentrated and dialyzed by tangential flow to ~500 ml, and nickel-agarose (Qiagen, Valencia, CA) was added in batch. The proteins were eluted from the Ni-NTA resin in 0.2 M imidazole in Hepes-buffered saline (HBS). The COOH-terminal hexa-histidine tags were removed by overnight digestion with carboxypeptidase-A (1:100) before purification. Both undigested and digested NPR were further purified by Mono-Q and Superdex-200 gel filtration fast protein liquid chromatography (Pharmacia). Both sedimentation equilibrium ultracentrifugation and gel filtration chromatography revealed that NPR-C exists as a dimer both in the absence and presence of ligand. As a final step, the proteins were concentrated by Centricon (Millipore, Bedford, MA) to ~15 mg/ml in HBS, sterile-filtered, and stored at 4°C.
28. Protein secreted from *D. melanogaster* are normally glycosylated at consensus asparagines-linked sites with high-mannose glycans. Insect cells do not process Asn-linked glycans into complex-type sugars. The recombinant NPR-C was thoroughly deglycosylated enzymatically with PNGase-F. The deglycosylation was monitored over the course of 72 hours at room temperature to ensure complete removal of the Asn-linked glycans, which proceeds slowly for the native protein because of the steric inaccessibility of the asparagines linkages. Deglycosylation at the three Asn-linked sites was obvious from the presence of a ladder of three bands on SDS gel, which collapsed to the lowest band over time. Moreover, this deglycosylated protein did not bind to con-A Sepharose. The deglycosylated NPR-C was repurified by gel filtration, which confirmed that it was not aggregated and was still folded and soluble. Native gel analysis of this deglycosylated protein revealed that it did not show band-shifting in the presence of NP hormones, indicating a loss of hormone-binding activity. This is consistent with functional studies of glycosylation mutants of NPR-A, -B, and GC-C that have lost activity. In addition, the inclusion of tunicamycin, an inhibitor of Asn-linked glycosylation, into the growth media of the NPR-C and NPR-A in *Drosophila* cells results in the inhibition of expression, suggesting a vital role for the carbohydrates in the folding of the protein.
29. J. E. Ladbury, B. Z. Chowdhry, *Chem. Biol.* **3**, 791 (1996).
30. The calorimetric titrations were carried out in a VP-ITC calorimeter (MicroCal, Northampton, MA) at 30°C (and 15°C for CNP), and the data were analyzed with the program Microcal Origin 5.0. The NPR-C protein was identical to that used for crystallization and was further purified by gel filtration chromatography immediately before the ITC experiments (NPR-C shows no tendency to aggregate at the conditions and temperature of the ITC experiments). The protein concentrations were determined with the bicinchoninic acid assay with bovine serum albumin as standard (Pierce, Rockford, IL). The concentration of the hormone-binding domain was calculated with a derived molecular weight of 48 kD. Peptide hormones (Bachem, Foster City, CA) were >99% pure and concentrations were determined based on the product data from the manufacturer. All the materials were resuspended in an identical lot of 150 mM NaCl and 10 mM Hepes (pH 7.2) for the experiments to control for buffer heat dilution effects. For all experiments, the receptor ECD was included in the sample cell at 1.5 and 3 μM concentration, and the hormones were added to the receptor from a concentrated stock (1 mg/ml) over the course of numerous injections to the point that the receptor was fully saturated with ligand. As a measure of the buffer heat dilution, the additional injections of peptide were made after receptor saturation for baseline subtraction. As a final control, at the conclusion of an experiment, the titrated receptor/hormone complexes in the ITC cell were injected over a gel filtration column to confirm complex formation and verify that the receptor had not aggregated over the course of the experiments. ITC titrations of a soluble extracellular domain of human NPR-B expressed from insect cells with CNP-22 confirms the 1:2 stoichiometry (X.-l. He, D.-c. Chow, K. C. Garcia, unpublished data).
31. J. Janin, *Structure* **5**, 473 (1997).
32. F. A. Quiocho, P. S. Ledvina, *Mol. Microbiol.* **20**, 17 (1996).
33. Supplementary Web material is available on Science Online at [www.sciencemag.org/cgi/content/full/293/5535/1657/DC1](http://www.sciencemag.org/cgi/content/full/293/5535/1657/DC1).
34. S. L. Mowbray, A. J. Bjorkman, *J. Mol. Biol.* **294**, 487 (1999).
35. T. Duda, R. M. Goracznik, R. K. Sharma, *Biochem. Biophys. Res. Commun.* **212**, 1046 (1995).
36. A. Wada et al., *Infect. Immun.* **64**, 5144 (1996).
37. A. M. Engel, J. R. Schoenfeld, D. G. Lowe, *J. Biol. Chem.* **269**, 17005 (1994).
38. M. Matsumura, D. H. Fremont, P. A. Peterson, I. A. Wilson, *Science* **257**, 927 (1992).
39. K. S. Misono, *Circ. Res.* **86**, 1135 (2000).
40. Single-letter abbreviations for the amino acid residues are as follows: A, Ala; C, Cys; D, Asp; E, Glu; F, Phe; G, Gly; H, His; I, Ile; K, Lys; L, Leu; M, Met; N, Asn; P, Pro; Q, Gln; R, Arg; S, Ser; T, Thr; V, Val; W, Trp; and Y, Tyr.
41. The following crystallographic programs and software were used: ALS-CRIP; [G. J. Barton, *Protein Eng.* **6**, 37 (1993)]; CCP4, AmoRe, MOSFLM, SCALA [*Acta Crystallogr. D* **50**, 760 (1994)]; MOLREP [V. Vagin, A. Teplyakov, *J. Appl. Crystallogr.* **30**, 1022 (1997)]; CNS [A. T. Brünger et al., *Acta Crystallogr. D* **54**, 905 (1998)]; BOBSCRIPT [R. M. Esnouf, *J. Mol. Graph. Model.* **15**, 133 (1997)]; RASTER3D [E. A. Merritt, M. E. P. Murphy, *Acta Crystallogr. D* **50**, 869 (1994)]; VMD [W. Humphrey, A. Dalke, K. Schulten, *J. Mol. Graphics* **14**, 33 (1996)]; MSMS; M. F. Sanner, J.-C. Spohner, A. J. Olson, *Biopolymers*, **38**, 305 (1996)]; Matthews Coefficient [B. W. Matthews, *J. Mol. Biol.* **33**, 491 (1968)]; PROCHECK [R. A. Laskowski, M. W. MacArthur, D. S. Moss, J. M. Thornton, *J. Appl. Crystallogr.* **26**, 283 (1993)]; and O [T. A. Jones, J. Y. Zhou, S. W. Cowan, M. Kjeldgaard, *Acta Crystallogr. A* **47**, 110 (1991)].
42. We thank D. Lowe, D. Goeddel, M. Davis, and I. Wilson for support and encouragement; F. van den Akker for discussions; and the staffs of the Stanford Synchrotron Radiation Laboratory and the Advanced Light Source-Berkeley for their assistance. X.L.H. is supported by fellowships from the California Cancer Research Program and American Heart Association, and K.C.G. is supported by the American Heart Association, R. W. Johnson-PRI, the Cancer Research Institute, and the Rita Allen, Frederick Terman, and Pew Scholar awards. Coordinates of unliganded and liganded NPR-C are available upon publication from the RCSB Protein Data Bank under accession codes 1JDN and 1JDP, respectively.

3 May 2001; accepted 6 July 2001